ChemPubSoc Europe

DOI: 10.1002/chem.201900244

CHEMISTRY A European Journal Communication

High-Pressure Chemistry | *Hot Paper*

Revisiting Bond Breaking and Making in $EuCo_2P_2$: Where are the Electrons?

Vincent Yannello,[a] Francois Guillou,[b, h] Alexander A. Yaroslavtsev,[c, d] Zachary P. Tener,[a] Fabrice Wilhelm,[b] Alexander N. Yaresko,[e] Serguei L. Molodtsov,[c, f, g] Andreas Scherz,[c] Andrei Rogalev,*[b] and Michael Shatruk*[a]

Abstract: X-ray absorption spectroscopy (XAS) was used to elucidate changes in the electronic structure caused by the pressure-induced structural collapse in $EuCo_2P_2$. The spectral changes observed at the L_3-edge of Eu and K-edges of Co and P suggest electron density redistribution, which contradicts the formal charges calculated from the commonly used Zintl–Klemm concept. Quantum-chemical calculations show that, despite the increase in the oxidation state of Eu and the formation of a weak P–P bond in the high-pressure phase, the electron transfer from the Eu 4f orbitals to the hybridized 5d and 6s states causes strengthening of the Eu–P and P–P bonds. These changes explain the increased electron density on P atoms, deduced from the P K-edge XAS spectra. This work shows that the formal electron counting schemes do not provide an adequate description of changes associated with phase transitions in metallic systems with substantial mixing of the electronic states.

In 1985, a seminal paper by Hoffmann and Zheng addressed chemical aspects of structural phase transitions in $ThCr_2Si_2$-type structures.[1] It was proposed that breaking and making the X–X bonds between the $[T_2X_2]$ layers (X = group 13–16 element; T = transition metal), separated by layers of alkali, alkali-earth, or rare-earth metal atoms (A), correlate with the filling of the transition metal d-band. Since then, such correlations have been the focus of many studies on structural, electronic, and magnetic phase transitions in this class of materials.[2]

The structural phase transitions in the $ThCr_2Si_2$-type materials involve the collapse or expansion of the structure along the tetragonal *c*-axis, parallel to the interlayer X–X bonds (Figure 1). Although quite a few examples of such transitions have been reported,[3] the direct experimental assessment of changes in the electron density redistribution between the A and $[T_2X_2]$ layers upon the formation and breaking of the X–X bonding interactions is largely lacking. Herein, we report the use of X-ray absorption spectroscopy (XAS) and quantum-chemical calculations to show that the changes in the electron distribution caused by the pressure-induced structural collapse

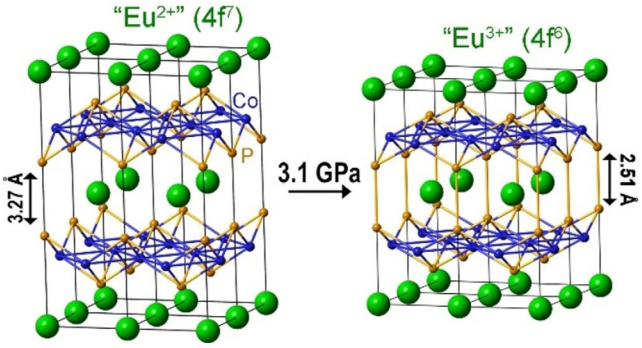

Figure 1. The normal and collapsed crystal structures of $EuCo_2P_2$, indicating the formal oxidation states of the Eu sites.

[a] *Dr. V. Yannello, Z. P. Tener, Prof. Dr. M. Shatruk*
Department of Chemistry and Biochemistry
Florida State University
95 Chieftan Way, Tallahassee, FL 32306 (USA)
E-mail: shatruk@chem.fsu.edu

[b] *Dr. F. Guillou, Dr. F. Wilhelm, Dr. A. Rogalev*
ESRF-The European Synchrotron
71 Avenue des Martyrs, 38000 Grenoble (France)
E-mail: rogalev@esrf.fr

[c] *Dr. A. A. Yaroslavtsev, Prof. Dr. S. L. Molodtsov, Dr. A. Scherz*
European XFEL GmbH
Holzkoppel 4, 22869 Schenefeld (Germany)

[d] *Dr. A. A. Yaroslavtsev*
National Research Nuclear University "MEPhI"
Kashirskoe shosse 31, 115409 Moscow (Russia)

[e] *Dr. A. N. Yaresko*
Max-Planck-Institut für Festkörperforschung
Heisenbergstraße 1, 70569 Stuttgart (Germany)

[f] *Prof. Dr. S. L. Molodtsov*
Institute of Experimental Physics
Technische Universität Bergakademie Freiberg
09599 Freiberg (Germany)

[g] *Prof. Dr. S. L. Molodtsov*
ITMO University
Kronverkskiy Prospect 49, 197101 St. Petersburg (Russia)

[h] *Dr. F. Guillou*
Present address: Inner Mongolia Key Laboratory for Physics and Chemistry of Functional Materials
Inner Mongolia Normal University
No 81 Zhaowuda Road, Hohhot (P. R. China)

Supporting information and the ORCID identification number(s) for the author(s) of this article can be found under: https://doi.org/10.1002/chem.201900244.

in $EuCo_2P_2$ defy the formal electron-counting rules commonly used for Zintl-like phases, including those that contain transition and rare-earth metals.[4]

$EuCo_2P_2$ undergoes a first-order transition, without the space group change (*I*4/*mmm*), from the normal to the collapsed $ThCr_2Si_2$-type structure at the critical pressure of 3.1 GPa at room temperature.[3c] The normal, low-pressure (LP) structure features a long P–P separation of 3.27 Å and Eu^{2+} oxidation state, whereas the collapsed, high-pressure (HP) structure exhibits a much shorter P–P distance of 2.51 Å and Eu^{3+} oxidation state.[3a,5] A traditional Zintl–Klemm electron counting approach[6] suggests the phosphorus oxidation state of −3 in the LP-$EuCo_2P_2$ (due to the octet rule and the lack of P–P bonding), and thus the charge balance considerations lead to the +2 oxidation state for cobalt. If one assumes the formation of a P–P bond in the HP-$EuCo_2P_2$ structure, the oxidation states of P and Co become −2 and +0.5, respectively. This formal treatment, however, hardly conveys the realistic physical picture in the metallic systems with strong covalent bonding, where electronic states of different elements are strongly mixed. When the difference in the electronegativity of T and X elements becomes relatively small, the validity of the simple charge distribution scheme becomes questionable. The electronegativity values for Co and P are 1.88 and 2.19, respectively.[7] Furthermore, the P–P distance of 2.51 Å observed in the HP-$EuCo_2P_2$ structure[3a] is still substantially longer than a typical P–P single bond (2.22 Å),[8] and thus the assumption about a pair of electrons being simply shared in the bond between the P atoms is also debatable.

To probe directly the changes in the electron density distribution of $EuCo_2P_2$ upon the structural phase transition, we carried out a pressure-dependent XAS study on this material, which was synthesized as reported previously.[9] The XAS experiments were performed at the L_3-edge of Eu and K-edges of Co and P. The XAS measurement at the K-edge of phosphorus using the diamond anvil cell (DAC) is not trivial, due to the relatively low photon energy of the K-edge (≈2.14 keV) that causes high absorption of X-rays by the DAC. Therefore, a dedicated HP setup was used,[10] which consisted of a fully perforated front diamond anvil with a hole diameter of 100 μm complemented by a 30-μm thick diamond disk to limit the X-ray absorption. The XAS signal was recorded as a fluorescence spectrum in the back-scattering geometry.[10]

We and others have previously demonstrated that above the critical pressure of 3.1 GPa the LP-$EuCo_2P_2$ phase transforms into the HP-$EuCo_2P_2$ phase, with the clear change in the oxidation state of Eu,[3c,9] which was also confirmed in the present experiments by the dramatic change in the XAS spectra observed at the Eu L_3-edge (Figure 2a). Based on these spectral changes, Eu undergoes a nearly complete conversion from the +2 to +3 formal oxidation state. In contrast, the Co K-edge spectra showed only minor changes under applied pressure (Figure 2b). Some broadening of the absorption features can be attributed to the increase in the metallic character of the Co electronic states as the pressure increases.

The observation of the increase in the Eu oxidation state and negligible spectral changes at the Co K-edge suggests that the pressure-induced structural collapse results in electron density redistribution from the Eu sites toward the P sites. Indeed, a striking change was observed in the P K-edge XAS spectra (Figure 2c). Above the critical pressure, the "white line" shifted to substantially higher energies, whereas the higher-energy part of the spectrum remained nearly unchanged. This is in contrast to the Eu L_3-edge, where the entire spectrum is shifted to higher energies due to the depopulation of the 4f orbitals and increased oxidation state. The character of the P K-edge absorption involves 1s→*n*p electronic excitations, and thus the spectral changes observed suggest filling of phosphorus p-states, since the "white-line" excitations to the empty p-states require higher energy (Figure S1 in Supporting Information). The change in the occupation of the phosphorus 3p states is also reflected in the decreased intensity of the "white line" at higher pressure, confirming the lesser number of holes in the 3p band in the collapsed HP phase. Similar changes in the XANES spectra, caused by changes in the population of the 3p band, have been observed at the sulfur K-edge for various sulfide minerals.[11] (A more detailed discussion of the changes in the P K-edge spectra is also provided in the Supporting Information.)

The observation of the increased electron density in the phosphorus 3p band is in striking contradiction to the purported pressure-induced −3→−2 change in the formal oxidation state on the P atoms, suggesting that the charge distribution scheme discussed above does not apply to the present system. The increase in the filling of p-states, however, makes sense, keeping in mind the increase in the Eu oxidation state

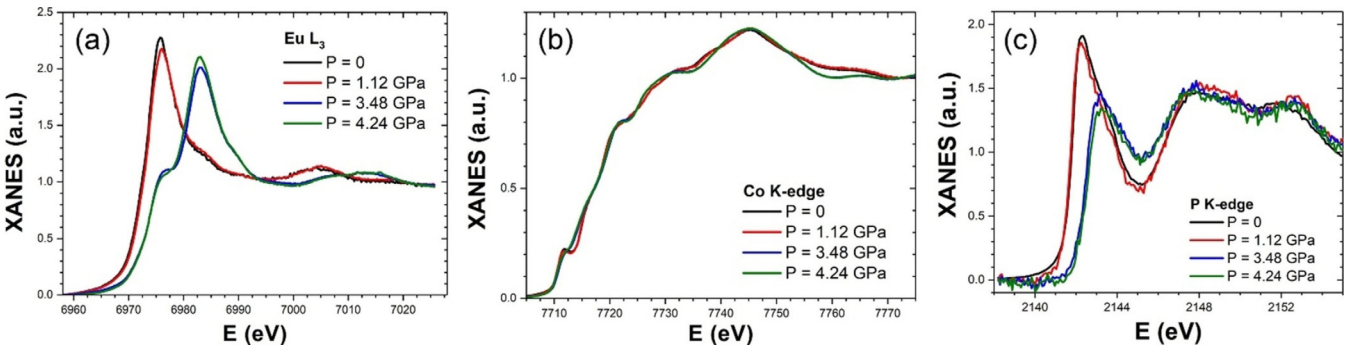

Figure 2. Pressure-dependent XAS spectra of $EuCo_2P_2$ collected at the Eu L_3-edge (a), Co K-edge (b), and P K-edge (c).

and only the minor changes in the Co K-edge spectra with pressure.

In order to understand the nature of the observed changes in the element-specific XAS spectra, we carried out quantum-chemical calculations on the LP and HP structures of $EuCo_2P_2$. The calculations were performed with LMTO[12] and VASP[13] computational packages, in order to ensure the reproducibility of results with different electronic structure codes (Figure S2).

A simple computational check for the charges on individual atoms is performing a Bader charge calculation.[14] Zero-flux electron density surfaces are generated, creating atom-centred regions. Integrating inside of these regions gives an approximate number of electrons associated with each atom, and thus the atomic charge. The results of such calculations for both the LP and HP structures, as well as the formal Zintl charges, are shown in Table 1. Upon going from the LP to HP structure, Eu experiences oxidation, as expected, although the change is not as severe, suggesting involvement of the Eu 6s and 5d orbitals. The Co and P, however, are both slightly reduced, by approximately the same amount. Importantly, the Bader charge on the P atom in the HP phase is only around −0.7, indicating a moderate extent of electron transfer from the more electropositive atoms. This finding is reasonable, given the relatively small electronegativity difference between Co (1.88) and P (2.19).

Table 1. Bader and Zintl charges for the LP- and HP-$EuCo_2P_2$.

	Bader charges		Zintl charges	
	Normal (LP)	Collapsed (HP)	Normal (LP)	Collapsed (HP)
Eu	+1.13	+1.50	+2	+3
Co	+0.04	−0.05	+2	+0.5
P	−0.61	−0.70	−3	−2

The charges calculated for the Eu site deserve some further discussion. They suggest that as the Eu atom is being oxidized, more electrons become available for bonding. As seven of the nine valence electrons in Eu^{2+} were treated as core f-orbitals, only two electrons remained as truly valence states. In Eu^{3+}, six electrons were placed in the core, with three valence electrons remaining. This means that in the LP-$EuCo_2P_2$, with the calculated +1.13 charge for Eu, 0.87 valence electrons are still assigned to Eu, whereas in the HP-$EuCo_2P_2$ the charge on Eu is +1.50, meaning that each Eu atom has 1.50 valence electrons. Such charge assignments are indirectly confirmed by XAS results. Due to the expected hybridization (bonding) between the P 3p-states and Eu 5d-states, the large shift in the P K-edge might indicate the filling of Eu valence states, whereas at the Eu L_3-edge this effect is "hidden" by the stronger Eu valence transition.

To better understand how the re-distribution of electrons upon the pressure-induced structural transition correlates with changes in the chemical bonding in $EuCo_2P_2$, we calculated Crystal Orbital Hamilton Population (COHP)[15] for the five shortest interatomic contacts, Eu–Co, Eu–P, Co–Co, Co–P, and P–P. The COHP curves (Figure 3) illustrate an energy-resolved bonding scheme, with positive and negative values representing bonding and antibonding states, respectively. As expected, the P–P contacts show a large increase in bonding when going from the normal to collapsed structure. Additionally, the Co–P curves are uniformly quite large. The Eu–Co and Eu–P curves also show sizable bonding contributions.

Negative integrated COHP (-ICOHP) values were calculated for all five contacts (Table 2) to ascertain the strength of the various contacts and their change upon increasing the pressure. The experimental bond lengths are also shown for reference. They correlate well with the calculated -ICOHP values, which reveal significant strengthening of the P–P bond and slight weakening of the Co–P and Co–Co bonds. Perhaps, the most interesting result is the strengthening of the Eu–Co and Eu–P bonding in the collapsed HP structure. The -ICOHP value for the Eu–P interaction is nearly as large as that for the P–P contact, that is, both Eu–P and P–P bonds are substantially strengthened in the HP structure as compared to the LP structure of $EuCo_2P_2$. Given the relative increase in the number of valence electrons on the Eu sites (see above), the increase in the Eu–Co and Eu–P bond strengths can be attributed to a greater filling of these bonding states.

Our findings suggest that the traditional use of formal charges to interpret the nature of the structural phase transition in $EuCo_2P_2$ is inappropriate. A physically more reasonable

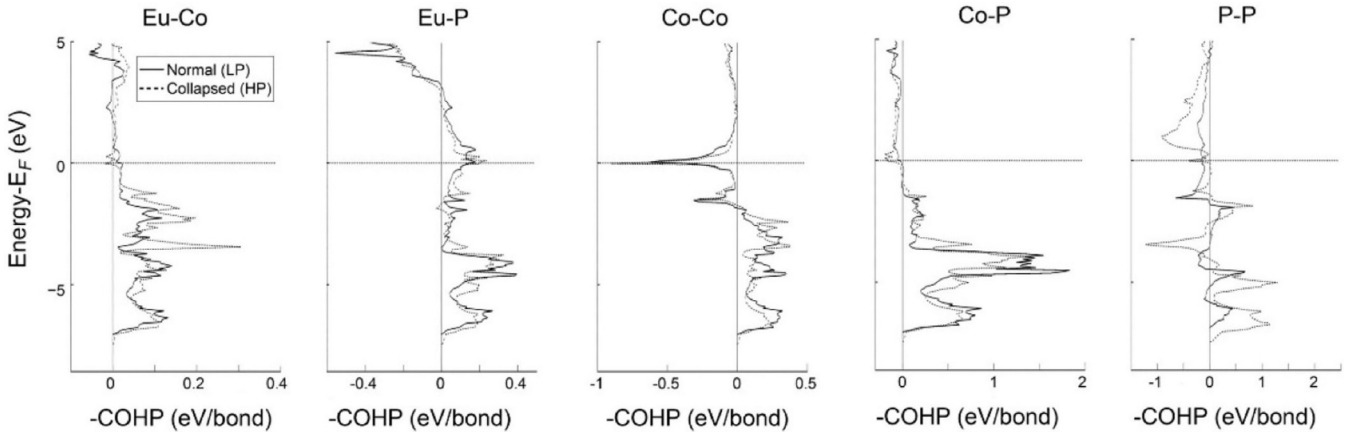

Figure 3. COHP curves for the Eu–Co, Eu–P, Co–Co, Co–P, and P–P interatomic contacts in the LP (solid line) and HP (dashed line) structures of $EuCo_2P_2$.

Table 2. Negative integrated COHP values for the five interatomic contacts in $EuCo_2P_2$. Experimental bond lengths are also shown for reference.

	−ICOHP [eV bond^{-1}]		Bond lengths [Å]	
	LP	HP	LP	HP
Eu–Co	0.42	0.64	3.33	3.09
Eu–P	0.84	1.26	3.12	3.01
Co–Co	0.87	0.46	2.65	2.73
Co–P	3.87	2.78	2.18	2.23
P–P	0.13	1.48	3.27	2.57

picture is offered by considering the delocalized nature of electrons (band structure) in this material. The calculation of the Bader charges and the strength of chemical bonding, while being semi-quantitative due to treating the Eu 4f-electrons as quasi-core, does reveal that the bonding in this compound has much larger contributions from covalent and metallic effects. This leads to the electron transfer from Eu core level into the Eu–P and P–P bonding, thus resulting in the slight reduction of phosphorus, in reversal to what would be expected from the use of the Zintl–Klemm electron counting scheme. Importantly, our theoretical treatment provides a satisfactory explanation to the pressure-induced changes observed in the experimental XAS spectra of $EuCo_2P_2$. Thus, while the Zintl–Klemm concept frequently serves as a useful guide, one should remember that it is not a reflection of the true electronic structure and charge distribution; the conclusions drawn from this concept can be misleading when applied to metallic materials, such as $EuCo_2P_2$, with strongly mixed electronic states.

Finally, we should point out that $EuCo_2As_2$ also undergoes a pressure-induced structural collapse with the critical pressure of $\approx$4.5 GPa at room temperature.[16] In this compound, however, the change in the Eu oxidation state is not as drastic[9] as seen in the case of $EuCo_2P_2$. We carried out XAS measurements on the L_3-edge of Eu and K-edges of Co and As and observed the same spectral changes as seen in $EuCo_2P_2$, albeit to a lesser extent (Figure S3). The theoretical treatment of $EuCo_2As_2$ is complicated by the homogeneous mixed valence in the HP phase,[9] but based on the similarity of spectral changes one can expect the same tendencies toward pressure-induced redistribution of electron density as those observed in $EuCo_2P_2$.

Experimental Section

X-ray absorption spectroscopy: A phase-pure sample of $EuCo_2P_2$ was synthesized as reported previously.[9] The XAS measurements were performed at the ESRF ID12 beamline (European Synchrotron Research Facility, France). A dedicated high-pressure diamond anvil cell (DAC) with a He gas-driven membrane optimized for the tender X-ray range has been used.[10] The DAC consisted of an asymmetric diamond anvil configuration, in which a fully perforated diamond, with a culet diameter of 600 μm, an opening angle of 2×15°, and a hole diameter of 100 μm (front anvil) was complemented by a 30-μm thick diamond disk to minimize the X-ray absorption. The back anvil was a full diamond with the same culet diameter of 600 μm. The gasket was made of stainless steel with an indented thickness of 90 μm and a hole diameter of 300 μm. A small pellet of pressed powder was loaded inside the cell, and He gas was used as the pressure-transmitting medium. The pressure was measured in situ using the luminescence of a ruby chip.

For the P K-edge, the X-ray source was the first harmonic of HELIOS-II-type helical undulator (HU-52), whereas for the Eu L_3-edge and Co K-edge it was the first harmonic of the APPLE-II type helical undulator (HU-38) in pure helical mode. The advantage of using helical mode is that the content of the higher order harmonics is strongly reduced, since only the fundamental harmonic is emitted on the undulator axis. The X-ray beam was monochromatized using a fixed-exit double-crystal monochromator equipped with a pair of Si(111) crystals. As focal system, sets of 2D parabolic Be lenses were used, with the possibility to focus the beam typically to 3(v)×30(h) μm even at the energies as low as 2.1 keV where a single lens was sufficient. The X-ray fluorescence signal from the sample was collected in the back-scattering geometry, through the thin diamond window, using an energy-resolved Si drift detector. All spectra have been corrected for re-absorption effects.

Quantum-chemical calculations: Non-spin polarized total energies, density of state (DOS) curves, crystal orbital Hamilton population (COHP) curves, and Bader charges were calculated for $EuCo_2P_2$. COHP curves were calculated using the Stuttgart TB-LMTO-ASA method,[12] whereas the Bader charges were calculated using the Vienna ab initio Simulation Package (VASP)[13] and the Bader program.[17] The DOS curves were calculated using both methods for comparison. Additional relativistic PY LMTO calculations were performed (results are provided in the Supporting Information, Figures S3 and S4) to verify the downfolding of the 4f electrons in Eu.[18] Atomic positions were taken from the experimentally determined crystal structures. PAW-PBE pseudopotentials were used for all elements for the VASP calculations, while Eu_2 and Eu_3 being used in the expanded and collapsed structures, respectively. Eu 4f electrons were treated as core for all calculations. Further computational details can be found in the Supporting Information.

Acknowledgements

This research was supported by the National Science Foundation (award DMR-1507233).

Conflict of interest

The authors declare no conflict of interest.

Keywords: high-pressure chemistry · mixed-valent compounds · phase transitions · X-ray absorption spectroscopy · Zintl phases

[1] R. Hoffmann, C. Zheng, *J. Phys. Chem.* **1985**, *89*, 4175–4181.
[2] a) R. T. Macaluso, B. K. Greve, *Dalton Trans.* **2012**, *41*, 14225–14235; b) X. Tan, Z. P. Tener, M. Shatruk, *Acc. Chem. Res.* **2018**, *51*, 230–239; c) D. Johrendt, C. Felser, O. Jepsen, O. K. Andersen, A. Mewis, J. Rouxel, *J. Solid State Chem.* **1997**, *130*, 254–265; d) R. Pöttgen, *Z. Anorg. Allg. Chem.* **2014**, *640*, 869–891; e) M. Shatruk, *J. Solid State Chem.* **2019**, https://doi.org/10.1016/j.jssc.2019.02.012.
[3] a) C. Huhnt, W. Schlabitz, A. Wurth, A. Mewis, M. Reehuis, *Phys. Rev. B* **1997**, *56*, 13796–13804; b) C. Huhnt, W. Schlabitz, A. Wurth, A. Mewis, M. Reehuis, *Physica B* **1998**, *252*, 44–54; c) M. Chefki, M. M. Abd-Elmeguid, H. Micklitz, C. Huhnt, W. Schlabitz, M. Reehuis, W. Jeitschko, *Phys. Rev. Lett.* **1998**, *80*, 802–805; d) W. Uhoya, G. Tsoi, Y. K. Vohra, M. A. McGuire, A. S. Sefat, B. C. Sales, D. Mandrus, S. T. Weir, *J. Phys. Condens.*

Matter **2010**, *22*, 292202; e) R. M. Bornick, A. M. Stacy, *Chem. Mater.* **1994**, *6*, 333 – 338.
[4] S. M. Kauzlarich, in *Chemistry, Structure, and Bonding of Zintl Phases and Ions* (Ed.: S. M. Kauzlarich), Wiley-VCH, Weinheim, **1996**, pp. 245 – 274.
[5] B. Ni, M. M. Abd-Elmeguid, H. Micklitz, J. P. Sanchez, P. Vulliet, D. Johrendt, *Phys. Rev. B* **2001**, *63*, 100102.
[6] G. J. Miller, in *Chemistry, Structure, and Bonding of Zintl Phases and Ions* (Ed.: S. M. Kauzlarich), Wiley-VCH, Weinheim, **1996**, pp. 1 – 59.
[7] L. C. Pauling, *The Nature of the Chemical Bond and the Structure of Molecules and Crystals. An Introduction to Modern Structural Chemistry*, 3rd ed., Cornell University Press, Ithaca, NY, **1960**.
[8] P. Pyykkö, *J. Phys. Chem. A* **2015**, *119*, 2326 – 2337.
[9] X. Tan, G. Fabbris, D. Haskel, A. A. Yaroslavtsev, H. Cao, C. M. Thompson, K. Kovnir, A. P. Menushenkov, R. V. Chernikov, V. O. Garlea, M. Shatruk, *J. Am. Chem. Soc.* **2016**, *138*, 2724 – 2731.
[10] F. Wilhelm, G. Garbarino, J. Jacobs, H. Vitoux, R. Steinmann, F. Guillou, A. Snigirev, I. Snigireva, P. Voisin, D. Braithwaite, D. Aoki, J. P. Brison, I. Kantor, I. Lyatun, A. Rogalev, *High Pressure Res.* **2016**, *36*, 445 – 457.
[11] R. Alonso Mori, E. Paris, G. Giuli, S. G. Eeckhout, M. Kavčič, M. Žitnik, K. Bučar, L. G. M. Pettersson, P. Glatzel, *Anal. Chem.* **2009**, *81*, 6516 – 6525.
[12] R. Tank, O. Jepsen, A. Burkhardt, O. K. Andersen, *The program TB-LMTO-ASA. Version 4.7*, Max-Planck-Institut fur Festkorperforschung, Stuttgart, **1999**.
[13] a) G. Kresse, J. Furthmüller, *Phys. Rev. B* **1996**, *54*, 11169 – 11186; b) G. Kresse, D. Joubert, *Phys. Rev. B* **1999**, *59*, 1758 – 1775.
[14] R. F. W. Bader, *Atoms in Molecules: A Quantum Theory*, Clarendon, Oxford, **1994**.
[15] R. Dronskowski, P. E. Blochl, *J. Phys. Chem.* **1993**, *97*, 8617 – 8624.
[16] M. Bishop, W. Uhoya, G. Tsoi, Y. K. Vohra, A. S. Sefat, B. C. Sales, *J. Phys. Condens. Matter* **2010**, *22*, 425701.
[17] W. Tang, E. Sanville, G. Henkelman, *J. Phys. Condens. Matter* **2009**, *21*, 084204.
[18] V. Antonov, B. Harmon, A. Yaresko, *Electronic Structure and Magneto-Optical Properties of Solids*, Kluwer Academic, Dordrecht, Boston, London, **2004**.

Manuscript received: January 16, 2019
Accepted manuscript online: February 4, 2019
Version of record online: February 21, 2019